Land-Sea Clutter Classification for Over-the-Horizon Radar via Dual Attention Aided Residual Neural Networks

1st Can Li
School of Automation
Northwestern Polytechnical University
Xi'an, China
lican@mail.nwpu.edu.cn

2nd Quan Pan
School of Automation
Northwestern Polytechnical University
Xi'an, China
quanpan@nwpu.edu.cn

3rd Zuowei Zhang
School of Automation
Northwestern Polytechnical University
Xi'an, China
zhangzuowei@nwpu.edu.cn

4th Zhunga Liu
School of Automation
Northwestern Polytechnical University
Xi'an, China
liuzhunga@nwpu.edu.cn

5th Xianglong Bai
School of Automation
Northwestern Polytechnical University
Xi'an, China
baixianglong@mail.nwpu.edu.cn

6th Kunpeng Pan
School of Automation
Northwestern Polytechnical University
Xi'an, China
pankunpeng@mail.nwpu.edu.cn

***Abstract*—Deep learning has been widely used in the field of radar image classification because of its powerful feature extraction capabilities. In the land-sea clutter classification of sky-wave over-the-horizon radar (OTHR), deep learning methods perform poorly due to the radar receiver noise and the ionosphere. Addressing this challenge, a dual attention aided residual neural networks (DAAResNet) is proposed for OTHR land-sea classification. Leveraging prior knowledge that land-sea clutter features predominantly cluster around the 0 Hz frequency, two attention mechanisms are introduced. Firstly, a channel attention module (CAM) is proposed, which directs the network's focus towards critical channels. Secondly, a frequency attention module (FAM) is proposed, which directs attention towards pivotal frequencies. The classification performance of DAAResNet is validated on the original dataset and the scarce dataset. Experimental results show that DAAResNet outperforms state-of-the-art methods.**

***Index Terms*—Clutter classification, channel attention module, frequency attention module, over-the-horizon radar (OTHR)**

I. Introduction

Sky-wave over-the-horizon radar (OTHR) is a crucial system for remote sensing [1]–[3]. Matching the results of land-sea clutter classification with geographic information can be used to calculate coordinate registration parameters for target localization. This method has the potential to improve the target localization accuracy at a minimal cost [4].

Many scholars have explored efficient and feasible methods for land-sea clutter classification, including model-driven methods and data-driven methods. Barnum *et al.* [5] proposed a coordinate registration method based on land-sea clutter classification, which constructed a clutter model for clutter classification. However, this method has issues with complex models and insufficient information. Cuccoli *et al.* [6]–[8] studied the method of coordinate registration using geomorphic structure in the OTHR detection area. However, it assumed that the OTHR transmitted a single pulse signal and only provided numerical simulation results. Cacciamano *et al.* [9] proposed a method for evaluating coordinate registration errors using a three-dimensional ray tracing algorithm. Holdsworth [10] proposed a coordinate registration method that utilizes the backscatter intensity of surface echoes to improve target positioning accuracy. While the cited literature utilizes geographic information for extracting coordinate registration parameters, it primarily focuses on performing coordinate registration through geographic coordinate matching, with a limited exploration into land-sea clutter.

Turley *et al.* [11] introduced the Bragg ratio as the ratio between the energy peak and the sub-peak frequency within the Doppler spectrum. This metric was employed to formulate a graph edge equation based on neighboring range-azimuth units. Weighted least squares were then utilized to solve this equation set for land-sea clutter classification. Jin *et al.* [12] introduced a support vector machine (SVM)-based method for land-sea clutter classification. This method involved training the SVM using three types of spectral features related to land-sea clutter and validating it with simulation data, achieving relatively good classification accuracy. The preceding land-sea clutter classification methods employed a feature extraction and classification separation approach, wherein land-sea clutter features were manually extracted and then fed into a classifier for classification. However, in the operational setting of OTHR, these methods exhibit shortcomings such as underutilization of features and low accuracy. Therefore, it is imperative to investigate a robust and highly accurate land-sea clutter classification method.

Deep convolutional neural networks (DCNNs) excel at extracting intricate features from data. With the rapid development of DCNNs in radar image processing, several

scholars have proposed land-sea clutter classification methods based on DCNNs. In [13], superior accuracy was attained by extracting potential features from land-sea clutter data compared to LMS and SVM algorithms. The classification accuracy remained consistently high, not falling below 95%, even across datasets with varying signal time widths and coherent integration numbers (CIN). Li *et al.* [4] proposed a cross-scale DCNNs land/sea clutter classification method based on the idea of algebraic multigrid and interpolation-related image downsampling. Zhang *et al.* [14] proposed a method called auxiliary classifier variational autoencoder generative adversarial network and assessed its impact as a data augmentation technique on the classification performance of sea-land clutter samples. Zhang introduced the triple loss adversarial domain adaptation network for cross-domain sea-land clutter classification. This network aligns the characteristics, instances, and categories of land-sea clutter across various domains to obtain domain-invariant features, thereby enhancing classification performance in cross-domain scenarios. The mentioned methods underwent validation using a land-sea clutter dataset featuring prominent semantic features, without considering the complexity of data in the actual work of OTHR.

The spectrum data is intricate and dynamic. Radar echo signals are often obscured by considerable receiver noise, compounded by congestion in high-frequency bands, which can lead to residual radio communication interference. Moreover, radar echo signals are susceptible to various influences, including time-varying ionospheric conditions characterized by multi-layer, inhomogeneous, and anisotropic properties, etc.. These factors can result in amplitude fluctuations, radio frequency (RF) interference, clutter spectrum broadening, multipath clutter spectra, and the disappearance of certain spectral features, etc.. Thus, considering the complexity of land-sea clutter data is imperative to enhance the generalization ability of the model.

This article introduces the attention mechanism for land-sea clutter classification in OTHR. In recent years, the attention mechanism has been widely used in various fields, including image classification [15], [16], natural language modeling [17], image segmentation [18], medicine [19], finance [20], etc.. Its success depends largely on a reasonable assumption that human vision can quickly filter out high-value information from a large amount of information, thus improving the efficiency and accuracy of intuitive information processing. Taking the OTHR Range-Doppler (RD) map as an example, as shown in Fig. 1, human experts quickly focus on areas near 0 Hz frequency, where land-sea features are evident, thus realizing the task of land-sea clutter classification. Inspired by this, we propose a dual attention aided residual neural networks (DAAResNet) for land-sea clutter classification. Our goal is to use the attention mechanism to enhance the representation ability of ResNet, so that ResNet can focus on the vicinity of 0 Hz frequency where the features are mainly concentrated in the OTHR spectrum data, while suppressing the background noise.

In experiment validation, we prepare two kinds of land-sea clutter datasets: the original dataset and the scarce dataset. Experimental results show that the DAAResNet outperforms the state-of-the-art methods. Furthermore, the generalization ability of the DAAResNet is verified based on the scarce dataset.

In summary, our main contributions are threefold.

1) The attention-based land-sea clutter classification method has not been considered in the literature. A novel ResNet architecture, namely, DAAResNet is proposed for landsea clutter classification.

2) The proposed DAAResNet generates attention maps along two independent dimensions—channel and frequency, sequentially. Subsequently, these attention maps undergo multiplication with the input feature maps to achieve adaptive refinement of features. Employing an attentional mechanism, the DAAResNet aims to enhance feature representation, suppressing background noise and thereby improving the performance of land-sea clutter classification. Notably, the DAAResNet contributes to the interpretability of land-sea clutter classification.

3) The proposed DAAResNet is evaluated under four data acquisition scenarios with different radar parameters. Experimental results show that the DAAResNet outperforms the state-of-the-art methods on the original dataset and the scarce dataset.

The remainder of this article is organized as follows. The preliminaries, including problem description and data preparation, are presented in Section II. In Section III, the proposed DAAResNet is described in detail. In Section IV, the effectiveness and superiority of the proposed method on the original dataset and the scarce dataset with rich data categories are verified. Section V draws conclusions and highlights some future works.

II. Problem Description and Data Preparation

In this section, we first introduce the semantic characterization of the OTHR RD map and then describe the diversity of the sea-land clutter data. At last, we construct the original dataset with rich semantic features according to different radar working parameters, ionospheric environment, weather, region, etc..

A. Land-Sea Clutter Classification

Classifying land-sea clutter allows for the determination of whether the source of each range-azimuth unit is land or sea. We employ RD spectrum data as input features for the DCNNs, as features in the frequency domain are more visible, distinguishable, and concentrated, as shown in Fig. 1. In accordance with prior knowledge [14], sea clutter presents itself as a pair of Bragg peaks on the Doppler spectrum, exhibiting symmetry at 0 Hz frequency in the absence of a frequency shift. Land clutter is represented by a single peak at 0 Hz frequency in the Doppler spectrum. Moreover, mixed clutter has the characteristics of both land and sea clutter. In addition, referring to [13], the amplitude of land clutter

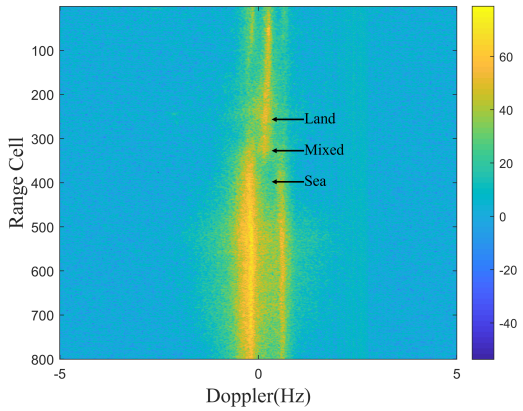

Fig. 1. RD map of OTHR in a fixed azimuth. Sea clutter appears as a pair of Bragg peaks in the Doppler spectrum and is symmetric at zero frequency if there is no frequency shift. Land clutter appears as a single peak at zero frequency in the Doppler spectrum. Mixed clutter has the characteristics of both land and sea clutter.

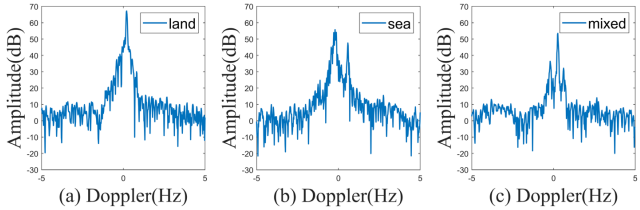

Fig. 2. Example of clutters. (a) land clutter. (b) sea clutter. (c) mixed clutter

is stronger than that of sea clutter because the scattering coefficient of land is larger than that of sea, as shown in Fig. 2. In this paper, we classify mixed clutter separately to prevent us from making fatal decisions when calculating coordinate registration parameters.

B. Data Preparation

Influenced by radar receiver noise, ionosphere, weather, sea state, etc., the radar echo signal may be contaminated by phenomena such as amplitude fluctuation, clutter spectrum broadening, multipath clutter spectrum, disappearance of part of the spectral features, and bending hooks. To ensure the diversity of the dataset, we collected the RD spectrum in different seasons and at different times of one day, and 200,000 range-azimuth units were selected by an expert system to constitute the original land-sea clutter dataset. The original dataset contains data affected by RF interference, amplitude fluctuations, Doppler shifts, and clutter spectral broadening, and does not contain data affected by multipath clutter spectra, loss of some spectral features, and bending hooks, while mixed clutter is separated into a separate category. Based on different CINs, we divide the data into four groups, i.e. Group A with 128 CIN, Group B with 256 CIN, Group C with 512 CIN, and Group D with 1024 CIN. Since our goal is to distinguish between sea clutter and land clutter whose energy lies in a narrow band under normal conditions, we choose the RD spectrum in the frequency interval [-5Hz, +5Hz], which helps to reduce the amount of computation, speeds up the convergence of the model, and prevents overfitting to some extent.

III. Dual Attention Aided Residual Neural Networks

In this section, we first present the framework of the proposed DAAResNet, then, we describe the channel attention module (CAM) and the frequency attention module (FAM).

A. Framework of the DAAResNet

The DAAResNet uses the ResNet model as the backbone network and adds an attention mechanism. The proposed module sequentially infers the attention map along two distinct dimensions, namely, channel and frequency, based on an intermediate feature map. Subsequently, this attention map is multiplied by the input feature map to achieve adaptive feature refinement.

We consider an intermediate feature map denoted by $\mathbf{F} \in \mathbb{R}^{C\times H\times W}$ as input to the attention module, where $\mathbb{R}$ is the field of real numbers, C is the number of channels, H and W are the height and width of the image, respectively. The attention mechanism generates a channel attention map $\mathbf{M}_\mathrm{c} \in \mathbb{R}^{C\times 1\times 1}$ and a frequency attention map $\mathbf{M}_\mathrm{f} \in \mathbb{R}^{1\times H\times W}$ in sequence. The attention process can be summarized as follows,

$$\begin{aligned}\mathbf{F}' &= \mathbf{M}_\mathrm{c}(\mathbf{F}) \otimes \mathbf{F},\\ \mathbf{F}'' &= \mathbf{M}_\mathrm{f}(\mathbf{F}') \otimes \mathbf{F}',\end{aligned} \tag{1}$$

where $\otimes$ denotes element-wise multiplication. During the process of multiplication, the attention values are replicated in a manner that aligns with their respective dimensions: channel attention values are replicated across the frequency dimension. The architecture of DAAResNet is shown in Fig. 3. In the following, we introduce the details of the channel attention module and the frequency attention module.

B. Channel Attention Module

CAM is an attention mechanism used to enhance model performance in deep learning. It is used to adjust the weights between different channels to improve the attention of the model to different feature channels. The channel attention mechanism is particularly useful in image processing and computer vision tasks, where it can help the network automatically learn the importance between channels, thereby improving the performance of the model. The aim is to automatically adjust the weight of the feature maps according to the importance of each channel, to better capture the correlation and feature importance between different channels. The architecture of the channel attention module is shown in Fig. 4. Note that in the convolution layers of CAM, to improve model performance at the cost of a small amount of computation, without parameter sharing.

To learn the importance weights of different channels, convolutional layers are introduced to capture the dependencies of channel aspects. This part includes two convolutional layers and two activation functions. To preserve the spatial structure

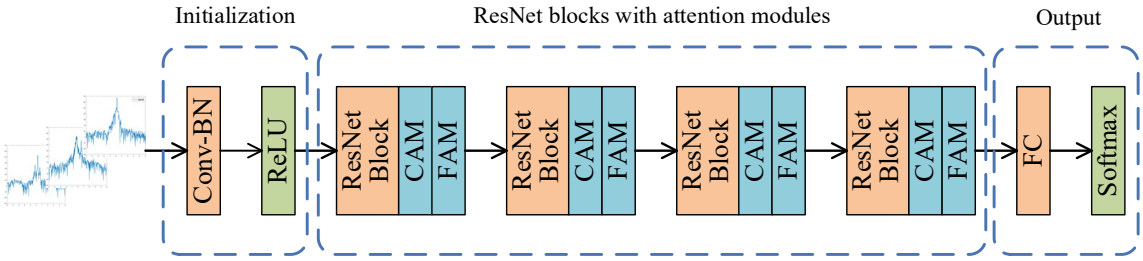

Fig. 3. Architecture of DAAResNet

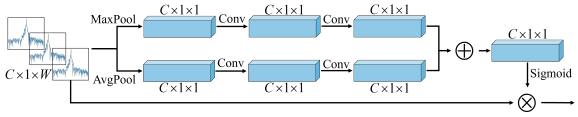

Fig. 4. Architecture of channel attention module

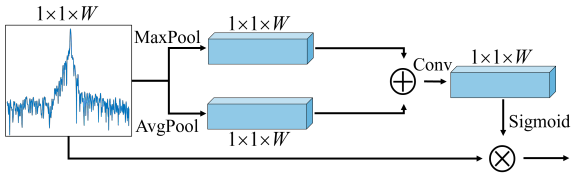

Fig. 5. Architecture of frequency attention module

of the input data, and reduce the number of parameters in the model, CAM uses convolutional layers instead of multi-layer perceptrons. The channel attention is computed as:

$$\begin{aligned} \mathbf{M}_{\mathrm{c}}^{\max}(\mathbf{F}) &= \delta\left(\mathbf{W}_4\left(\varphi\left(\mathbf{W}_3 * \mathbf{F}_{\mathrm{avg}}^{\mathrm{c}}\right)\right)\right), \\ \mathbf{M}_{\mathrm{c}}^{\mathrm{avg}}(\mathbf{F}) &= \delta\left(\mathbf{W}_2\left(\varphi\left(\mathbf{W}_1 * \mathbf{F}_{\max}^{\mathrm{c}}\right)\right)\right), \\ \mathbf{M}_{\mathrm{c}}(\mathbf{F}) &= \mathbf{M}_{\mathrm{c}}^{\max}(\mathbf{F}) + \mathbf{M}_{\mathrm{c}}^{\mathrm{avg}}(\mathbf{F}), \end{aligned} \tag{2}$$

where φ is the ReLU function, δ is the Sigmoid function, $\mathbf{W}_1$ and $\mathbf{W}_2$ are the convolution kernels of the first layer, $\mathbf{W}_3$ and $\mathbf{W}_4$ is the convolution kernels of the second layer. $\mathbf{M}_{\mathrm{c}}^{\max}(\mathbf{F})$ represent the channel max pooling attention map, $\mathbf{M}_{\mathrm{c}}^{\mathrm{avg}}(\mathbf{F})$ represent the channel average pooling attention map. $\mathbf{F}_{\mathrm{avg}}^{\mathrm{c}}$ and $\mathbf{F}_{\max}^{\mathrm{c}}$ represent the average pooling and max pooling operations in the channel attention module, respectively.

C. Frequency Attention Module

In traditional DCNNs, after using stacked convolution, pooling, and other calculations, the depth of the feature map increases, the size of the feature map decreases, and the receptive field of the convolution also increases. However, the position relationship of each data is always unchanged, and each position has the same impact on the result. The FAM can generate the weights for the frequency domain for the problem that different frequency regions in land-sea clutter have different degrees of importance for classification tasks. The region near 0 Hz frequency contains more abundant feature information and has a more critical impact on the classification results, so it needs to be given more attention. Other frequency domain regions may contain no or only a small amount of feature information, and have little influence on the classification results, so they can be given less attention.

The frequency attention module aggregates the information of the feature map through two pooling operations to generate two 1-D arrays. And then, frequency attention value is obtained by standard concatenation and convolution. The frequency attention is computed as:

$$\mathbf{M}_{\mathrm{f}}(\mathbf{F}) = \delta\left(f\left(\mathbf{F}_{\mathrm{avg}}^{\mathrm{f}} + \mathbf{F}_{\max}^{\mathrm{f}}\right)\right) \tag{3}$$

where the function f represents the convolution operation and δ is the Sigmoid function. $\mathbf{F}_{\mathrm{avg}}^{\mathrm{f}}$ and $\mathbf{F}_{\max}^{\mathrm{f}}$ representing the average pooling feature and the maximum pooling feature, respectively. The architecture of the channel attention module is shown in Fig. 5.

IV. Experiments

In this section, we verify the effectiveness of the proposed DAAResNet on the original land-sea clutter dataset and the scarce land-sea clutter dataset. The purpose of experiments on scarce dataset is to demonstrate the strong generalization ability of DAAResNet.

A. Data Description and Experimental Setup

To verify the effectiveness of DAAResNet, we adopt the land-sea clutter dataset containing rich semantic information, which is the spectrum data obtained by OTHR, as the original dataset. To ensure the diversity of the dataset, in addition to the samples with obvious semantic characteristics of the land-sea clutter, the dataset also contains samples with relatively poor ionospheric conditions or complex environments, such as RF interference, amplitude fluctuations, Doppler shifts, and clutter spectral broadening samples. Based on different CINs, the original dataset is divided into four groups, each group contains 50,000 samples of land-sea clutter. Taking Group A as an example, the dataset is randomly split into 70% as training set, and 30% as test set.

In addition, we construct scarce datasets based on the original dataset, where the test data is consistent with the original test data, and only partial samples of one or more categories are excluded from the original training data, as shown in Table I.

The experimental environment of the proposed DAAResNet is shown in Tabel II. To alleviate the effects of random initialization on the performance, all the experiments are repeatedly implemented 10 times, and the average performance

TABLE I
PERCENTAGE OF DIFFERENT CATEGORIES OF TRAINING DATA IN THE SCARCE DATASET

No.	Land	Sea	Mixed
scarce dataset-1	50%	50%	50%
scarce dataset-2	30%	30%	30%
scarce dataset-3	20%	20%	20%

TABLE II
EXPERIMENT ENVIRONMENT

Environment	Version
System	Windows10(64-bit)
GPU	NVIDIA GeForce RTX 3090
CUDA	11.6
python	3.9.0(in Anaconda 4.11.0)
torch	1.11.0
torchvison	0.12.0
NumPy	1.22.3
matplotlib	3.5.1

TABLE III
HYPERPARAMETER CONFIGURATION OF DAARESNET FOR LAN-SEA CLUTTER CLASSFICATION

Configuration	Default
Training Epoch	15
BatchSize	32
Learning Rate	0.001
Beta1	0.5
Beta2	0.999
Weight Initialization	-

is recorded. To verify the superiority of the proposed DAAResNet, we select four state-of-the-art methods for comparison, including ResNet18 with convolutional block attention module (CBAM-ResNet18) [15], ResNet18 [14], DCNNs [14] and SVM [12]. To be fair, the datasets and hyperparameters of all deep methods are consistent with DAAResNet, as shown in Table III.

The land-sea clutter is 1-D data, and the dataset is relatively small. At the same time, due to the limitation of computing resources, ResNet18 is used as the backbone network for DAAResNet and CBAM-ResNet18. For large datasets, DAAResNet can use ResNet34, ResNet50, and ResNet101 as the backbone network. The architecture of ResNet18 is shown in Fig. 6. The ResNet18 main structure consists of a convolutional layer, four residual block groups, and a fully connected layer. The batch sample training method is adopted in the experiment, and the number of samples in each batch is 32. The model performs 15 iterations of parameter updates on the training data. The adaptive moment estimation (Adam) method is used to optimize the loss function, the learning rate is set to 0.001, the Beta1 is set to 0.5, and the Beta2 is set to 0.999. The convolution kernel size of convolutional layer 1 is 1x5, the number is 64, and the step size is 2. The four residual block groups have the same structure, and each residual block group is composed of two residual blocks. The first residual block includes a convolution layer with a convolution kernel size 1x5 and step size 2, a convolution layer with convolution kernel size 1x5 and step size 1, and a shortcut connection. The second residual block includes two convolutional layers of size 1x5, step size 1, and a shortcut connection. The number of convolution kernels in the convolutional layer within each residual block group is the same, and the number of convolution kernels in the four residual block group convolutional layers is 64, 128, 256, and 512, respectively. Each convolutional layer in the model is connected with a Batch Normalization layer and a ReLU activation function. The Batch Normalization layer alleviates overfitting, and the RELU activation function makes full use of the gradient information to ensure the continuous convergence of the model.

B. Classification Accuracy Analysis

Table IV lists the classification accuracy of five different methods on the original sea-land clutter dataset. It can be seen that DAAResNet18 shows the best performance in all groups, with accuracies over 99%. The DAAResNet18 training accuracy curve is shown in Fig. 10, and the loss curve is shown in Fig. 11, it can be seen that the training of DAAResNet18 is stable and converges rapidly. In contrast, the classification accuracy of CBAM-ResNet18 is not lower than 98%. The reason is that, although the classifier structure of CBAM-ResNet18 has advantages over the remaining three methods on four different sets of land and sea clutter data sets, DAAResNet18 compares better with CBAM-ResNet18. Compared with ResNet18 and DCNNs, DAAResNet18 has about 2% higher classification accuracy on all datasets with different CINs.

The classification accuracies of the five different methods on the three scarce land-sea clutter datasets are presented in Fig. 7, Fig. 8, and Fig. 9, respectively. It can be seen that DAAResNet18 performs optimally on all three scarce datasets. On scarce dataset-3, which has the least amount of train data, DAAResNet18 still maintains a classification accuracy of no less than 93%. The experimental results show that although the classification performance of CBAM-Resnet18 outperforms the other three methods on three different scarce datasets, DAAResNet18 outperforms CBAM-Resnet18. Although ResNet18 has a classification accuracy of no less than 95% in scarce dataset-1, it performs poorly on scarce dataset-2 and scarce dataset-3. As the number of samples in the training data decreases, the classification accuracy of DCNNs and SVMs decreases rapidly.

C. Attention Mechanism Analysis

We visualize the input and output of the attention module, as shown in Fig. 12, to intuitively analyze the role of the attention module in the classification task of DAAResNet. Fig. 12 (a) and Fig. 12 (c) are the inputs of the attention module, Fig. 12 (b) and Fig. 12 (d) are the outputs of the attention module. With the forward propagation of the network, the

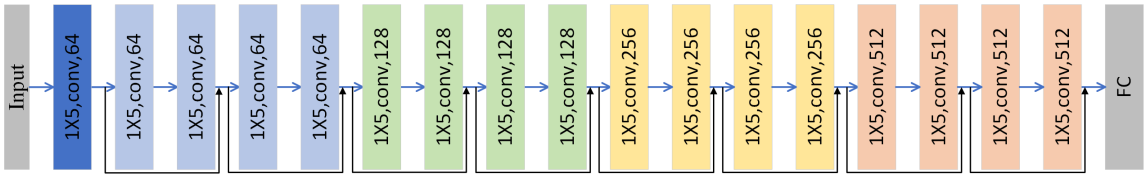

Fig. 6. Network structure of ResNet18 for land-sea clutter classification.

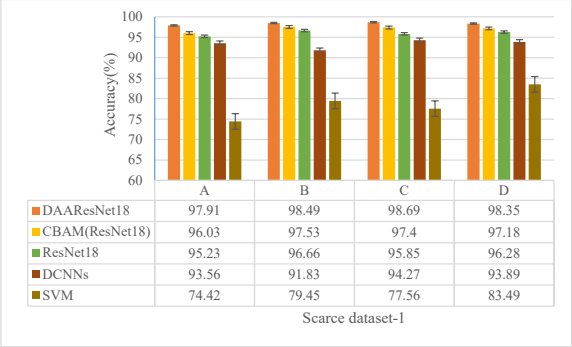

Fig. 7. Classification accuracy(%) of different compared methods on the scarce dataset-1

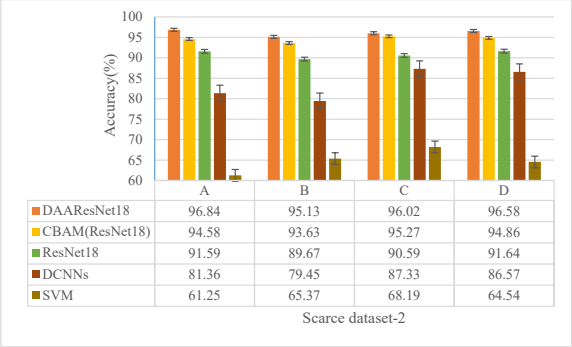

Fig. 8. Classification accuracy(%) of different compared methods on the scarce dataset-2

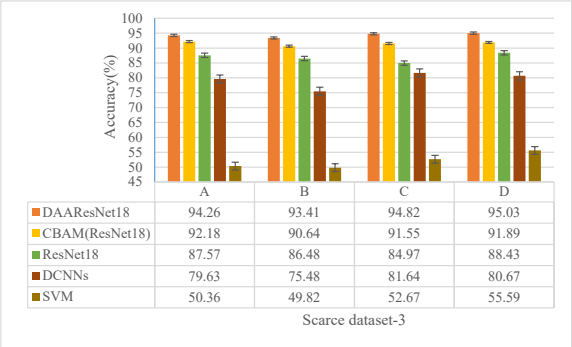

Fig. 9. Classification accuracy(%) of different compared methods on the scarce dataset-3

scale of the land-sea clutter continues to shrink, and the attention module continues to focus on the region near the

TABLE IV
CLASSIFICATION ACCURACY(%) OF DIFFERENT COMPARED METHODS ON THE ORIGINAL DATASET

Classifiers	A	B	C	D
DAAResNet18	**99.60**	**99.64**	**99.12**	**99.43**
CBAM(ResNet18)	98.60	98.13	98.66	98.73
ResNet18	97.65	98.02	97.43	98.22
DCNNs	96.97	97.14	96.65	96.55
SVM	85.69	88.57	89.03	91.61

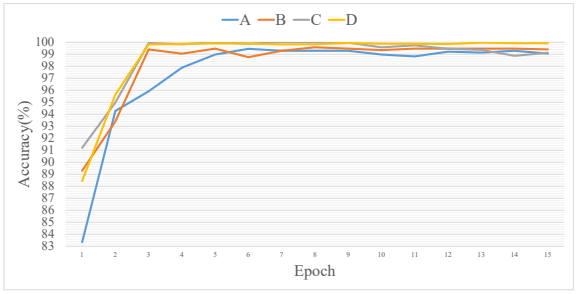

Fig. 10. Classification accuracy curve of DAAResNet18 for original dataset

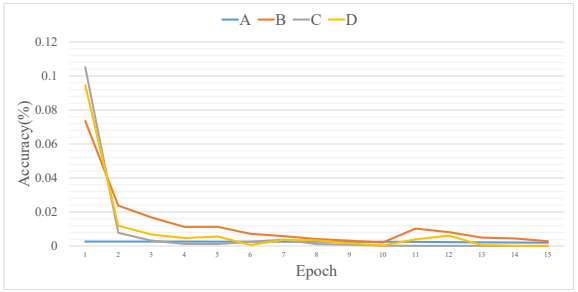

Fig. 11. Loss curve of DAAResNet18 for original dataset

0 Hz frequency, gradually increasing the weight size of this region while weakening other regions. As shown in Fig. 12 (a) and Fig. 12 (c), background noise is effectively suppressed. The application of the attention module in DAAResNet helps to mitigate the distortion phenomenon of land-sea clutter under RF interference, etc..

V. CONCLUSION

Inspired by the attention mechanism and the semantic information of OTHR spectrum data, a novel attention network, namely DAAResNet, is proposed. Experimental results show that DAAResNet has stronger classification performance on the land-sea clutter dataset, compared with the state-of-the-art classification methods. The DAAResNet uses the attention

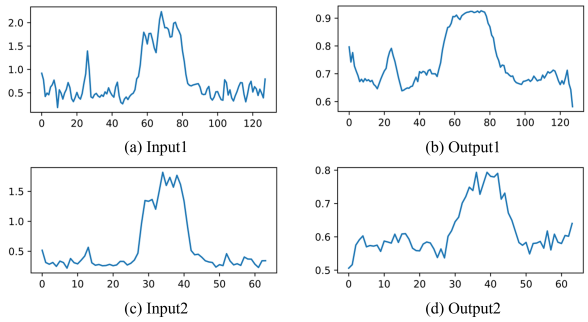

Fig. 12. Example of attention visualization.

mechanism to constrain the learning of the deep network and improve the interpretability of the classification results.

In future work, we plan to study the effects of different radar parameters, ionospheric conditions and environmental factors on land-sea clutter classification performance.

REFERENCES

[1] Z. Guo, Z. Wang, Y. Hu, Q. Pan, and J. Zhang, "Othr multipath tracking with correlated virtual ionospheric heights," in *2018 21st International Conference on Information Fusion (FUSION)*, 2018, pp. 2078–2082.

[2] L. Guo, J. Lan, and X. R. Li, "Multitarget tracking using over-the-horizon radar," in *2018 21st International Conference on Information Fusion (FUSION)*, 2018, pp. 24–31.

[3] B. Yang, J. Wang, W. Wang, and S. Wei, "Multipath generalized labeled multi-bernoulli filter," in *2018 21st International Conference on Information Fusion (FUSION)*, 2018, pp. 1423–1429.

[4] C. Li, Y. Zhang, Z.-f. Wang, K. Lu, and Q. Pan, "Cross-scale land/sea clutter classification method for over-the-horizon radar based on algebraic multigrid," *ACTA ELECTONICA SINICA*, vol. 50, no. 12, p. 3021, 2022.

[5] J. R. Barnum and E. E. Simpson, "Over-the-horizon radar target registration improvement by terrain feature localization," *Radio Science*, vol. 33, no. 4, pp. 1077–1093, 1998.

[6] F. Cuccoli, L. Facheris, D. Giuli, and F. Sermi, "Over the horizon sky-wave radar: simulation tool for coordinate registration method based on sea-land transitions identification," in *2009 European Radar Conference (EuRAD)*. IEEE, 2009, pp. 208–211.

[7] F. Cuccoli, F. Sermi, L. Facheris, and D. Giuli, "Sea-land transitions identification for coordinate registration of over the horizon sky-wave radar: numerical model for performance analysis," in *11-th INTERNATIONAL RADAR SYMPOSIUM*. IEEE, 2010, pp. 1–4.

[8] F. Cuccoli, L. Facheris, and F. Sermi, "Coordinate registration method based on sea/land transitions identification for over-the-horizon sky-wave radar: Numerical model and basic performance requirements," *IEEE Transactions on Aerospace and Electronic Systems*, vol. 47, no. 4, pp. 2974–2985, 2011.

[9] A. Cacciamano, A. Capria, D. Olivadese, F. Berizzi, E. Dalle Mese, F. Cuccoli *et al.*, "A coordinate registration technique for oth sky-wave radars based on 3d ray-tracing and sea-land transitions," *Progress In Electromagnetics Research*, vol. 147, 2012.

[10] D. A. Holdsworth, "Skywave over-the-horizon radar track registration using earth surface and infrastructure backscatter," in *2017 IEEE Radar Conference (RadarConf)*. IEEE, 2017, pp. 0986–0991.

[11] M. Turley, R. Gardiner-Garden, and D. Holdsworth, "High-resolution wide area remote sensing for hf radar track registration," in *2013 International Conference on Radar*. IEEE, 2013, pp. 128–133.

[12] Z. L. Jin, Q. Pan, C. H. Zhao, and W. T. Zhou, "Svm based land/sea clutter classification algorithm," *Applied Mechanics and Materials*, vol. 236, pp. 1156–1162, 2012.

[13] C. Li, Z. Wang, Z. Zhang, H. Lan, and K. Lu, "Sea/land clutter recognition for over-the-horizon radar via deep cnn," in *2019 International Conference on Control, Automation and Information Sciences (ICCAIS)*. IEEE, 2019, pp. 1–5.

[14] X. Zhang, Z. Wang, K. Lu, Q. Pan, and Y. Li, "Data augmentation and classification of sea-land clutter for over-the-horizon radar using acvaegan," *IEEE Transactions on Geoscience and Remote Sensing*, 2023.

[15] S. Woo, J. Park, J.-Y. Lee, and I. S. Kweon, "Cbam: Convolutional block attention module," in *Proceedings of the European conference on computer vision (ECCV)*, 2018, pp. 3–19.

[16] R. Hang, Z. Li, Q. Liu, P. Ghamisi, and S. S. Bhattacharyya, "Hyperspectral image classification with attention-aided cnns," *IEEE Transactions on Geoscience and Remote Sensing*, vol. 59, no. 3, pp. 2281–2293, 2020.

[17] Z. Niu, G. Zhong, and H. Yu, "A review on the attention mechanism of deep learning," *Neurocomputing*, vol. 452, pp. 48–62, 2021.

[18] B. Chen, Y. Liu, Z. Zhang, G. Lu, and A. W. K. Kong, "Transattunet: Multi-level attention-guided u-net with transformer for medical image segmentation," *IEEE Transactions on Emerging Topics in Computational Intelligence*, 2023.

[19] S. Harrer, "Attention is not all you need: the complicated case of ethically using large language models in healthcare and medicine," *EBioMedicine*, vol. 90, 2023.

[20] R. Khalfaoui, G. Gozgor, and J. W. Goodell, "Impact of russia-ukraine war attention on cryptocurrency: Evidence from quantile dependence analysis," *Finance Research Letters*, vol. 52, p. 103365, 2023.